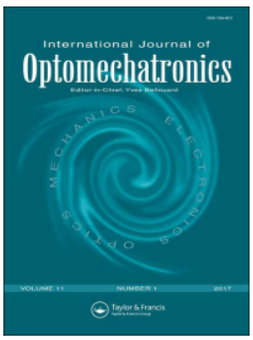

International Journal of Optomechatronics

ISSN: (Print) (Online) Journal homepage: https://www.tandfonline.com/loi/uopt20

Pyro-phototronic effect enhanced self-powered photodetector

Qi Li, Zhou Li & Jianping Meng

To cite this article: Qi Li, Zhou Li & Jianping Meng (2022) Pyro-phototronic effect enhanced self-powered photodetector, International Journal of Optomechatronics, 16:1, 1-17, DOI: 10.1080/15599612.2022.2051649

To link to this article: https://doi.org/10.1080/15599612.2022.2051649

Published online: 05 Apr 2022.

INTERNATIONAL JOURNAL OF OPTOMECHATRONICS
2022, VOL. 16, NO. 1, 1–17
https://doi.org/10.1080/15599612.2022.2051649

Pyro-phototronic effect enhanced self-powered photodetector

Qi Li[a,b], Zhou Li[a,b,c,d], and Jianping Meng[a,d]

[a]CAS Center for Excellence in Nanoscience, Beijing Key Laboratory of Micro–Nano Energy and Sensor, Beijing Institute of Nanoenergy and Nanosystems, Chinese Academy of Sciences, Beijing, P. R. China; [b]College of Chemistry and Chemical Engineering, Center on Nanoenergy Research, Guangxi University, Nanning, P. R. China; [c]Institute for Stem Cell and Regeneration, Chinese Academy of Sciences, Beijing, P. R. China; [d]School of Nanoscience and Technology, University of Chinese Academy of Sciences, Beijing, P. R. China

ABSTRACT

Pyro-phototronic effect has attracted much attention in fabricating self-powered high-performance photodetectors because of the significant enhancement by modulating the separation, transportation, and extraction of photo-generated electron-hole pairs in optoelectronic processes. This review highlights the advances in fabricating pyro-phototronic effect enhanced photodetectors. The fundamental research on the enhanced mechanism is discussed. Various device structures and figure of merit are summarized to demonstrate the improvement of performance by pyro-phototronic effect. Synergetic effects dominated by pyro-phototronic effect are also discussed to show their great potential and the universality of applying pyro-phototronic effect in photodetection. Finally, an outlook is delivered, and future research directions and challenges are discussed.

KEYWORDS

Pyro-phototronic effect; LSPR; piezo-phototronic effect; ferroelectricity; photodetector

1. Introduction

Photodetectors are in urgent demand in various fields such as military, astronomy, industrial production, medicine, and environmental monitoring. Its rapid development has also significantly made the human life more convenient. According to the bandgap of the sensing material, the photodetector can detect different wavelengths of light, such as ultraviolet, visible, and near-infrared light. Narrow bandgap semiconductors are always utilized as infrared photodetectors, such as Cu_2O, PbS, CuO, etc.[1–3] Besides, wide bandgap semiconductor materials are suitable for ultraviolet photodetectors, including ZnO, TiO_2, diamond, GaN, etc.[4–7] To date, there are a lot of high-performance photodetectors that have been reported to operate in the range from UV to IR.[8–9]

The photoelectric performance of photodetectors relates to the behaviors of the photo-generated electron-hole pairs involved in photoelectric conversion processes. The photoelectric conversion from optical signals to electrical signals through semiconductor-based photodetectors concerns a four-step process: [10](1) generation of the photo-generated electron-hole pairs, (2) separation of the photo-generated electron-hole pairs, (3) transportation of the photo-generated electron-hole pairs, (4) extraction of the photo-generated electron-hole pairs. A physical mechanism that can infect the four steps will have a significant effect on the performance of photodetectors. Pyro-phototronic effect is proposed to tune the separation, transportation, and extraction of

CONTACT Jianping Meng mengjianping@binn.cas.cn CAS Center for Excellence in Nanoscience, Beijing Key Laboratory of Micro–Nano Energy and Sensor, Beijing Institute of Nanoenergy and Nanosystems, Chinese Academy of Sciences, Beijing, P. R. China

Nomenclature

Cu_2O	Cuprous oxide	I	Iodine
PbS	Lead sulfide	MWs	Microwires
CuO	Cupric oxide	LDR	Linear dynamic range
ZnO	Zinc oxide	Ga	Gallium
TiO_2	Titanium dioxide	NPs	Nanoparticles
GaN	Gallium nitride	Si	Silicon
UV	Ultraviolet	LSPR	Localized surface plasmon resonance
IR	Infrared	NW	Nanowire
CdS	Cadmium sulfide	BTO	Barium titanate
P_s	Spontaneous polarization	Al_2O_3	Aluminum trioxide
I_p	Pyroelectric current	AR	Antireflection
PEC	Photoelectrochemical	SnS	Stannous sulfide
$BaTiO_3$	Barium titanate	ITO	Indium tin oxide
NW	Nanowire	FPV	Ferroelectric photovoltaic effect
NIR	Infrared	Pt	Platinum
ZnTe	Zinc telluride	$TmFeO_3$	Thulium ferrum oxide
V2O5	Vanadium pentoxide	$BiFeO_3$	Bismuth ferrum oxide
Ag	Silver	n-uLi	N-butyllithium
NiO	Nickel oxide	CuSCN	Cuprous thiocyanate
NRs	Nanorods	bR	Bacteriorhodopsin
PEDOT	Poly(3,4-ethylenedioxythiophene)	$MAPbI_3$	Methylammonium lead iodide
PSS	Poly(styrene sulfonic acid)	CMOS	Complementary metal oxide semiconductor
F	Fluorine	TiN	Titanium nitride
Cl	Chlorine		
Br	Bromine		

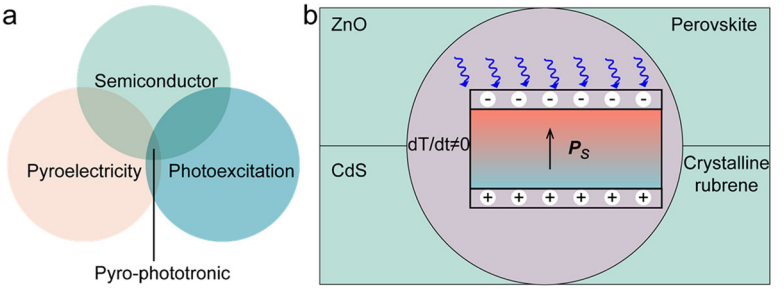

Figure 1. (*a*) Origination of pyro-phototronic effect. (*b*) Materials for pyro-phototronic effect and schematic pyroelectric effect.

photo-generated electron-hole pairs in optoelectronic processes recently, which couples pyroelectric effect and photoexcitation in a pyroelectric semiconductor (Figure 1(*a*)). Those materials that have been studied as having pyro-phototronic effect are mainly ZnO, CdS with wurtzite structure, perovskites, some organic materials such as crystalline rubrene (Figure 1(*b*)). These materials display pyroelectric effect mainly owing to noncentral symmetric crystal structures and thus can convert the temperature fluctuations (dT/dt) into electric signals. Temperature raises as the materials are illuminated under light, resulting in the change of spontaneous polarization (P_s). As a result, the bonding free charges (ions or electrons, which are called pyroelectric charges) on the charged surface at the two polar ends of crystal will be released, and the pyroelectric current (I_p) can be detected in the external circuit. The pyroelectric field produced by the primary and secondary pyroelectric effect will contribute to separating charge-carrier at the interface and prevent photo-generated electron-hole pairs from recombining in the crystal.[11] Moreover, the pyroelectric charges at a heterojunction can modulate the energy band of the semiconductor and the built-in potential.[12] In a word, the light-induced pyroelectric effect can promote the

performance of a photodetector and this mechanism is called pyro-phototronic effect. In addition, pyroelectric current can be expressed as $I_p = pA\ (\mathrm{d}T/\mathrm{d}t)$, where A and p are the electrode area and the pyroelectric coefficient, respectively. From the above formula, it can be seen that the pyroelectric current can be enhanced through improving the variation rate of temperature.[13]

Pyro-phototronic effect enhanced photodetectors have another key feature: they are self-powered photodetectors without applying bias. Self-powered photodetectors offer the advantages of low weight, small size, and low energy consumption, which are beneficial for wire-free environmental sensing, chemical/biological sensing, and in-situ medical monitoring. Self-powered photodetectors can be categorized into three kinds: p–n junction photodetectors,[14] Schottky junction photodetectors,[15] and photoelectrochemical-type (PEC-type) photodetectors.[16]

Here, we provide a comprehensive review of state-of-the-art research, which highlights pyro-phototronic effect for enhancing the performance of self-powered photodetectors. The narration stems from the pyro-phototronic effect in diverse photodetectors based on ZnO, $BaTiO_3$, CdS, and so on. Then, coupling pyro-phototronic effect among piezoelectricity, ferroelectricity, localized surface plasmon resonance (LSPR), and so on is summarized and discussed here. Finally, we conclude this article with some perspectives and outlooks on this new trend in the sensing field.

2. Pyro-phototronic effect in ZnO-based photodetectors

The original pyro-phototronic effect was uncovered by wang et al. [11] and has been developed to the point where the theory has taken shape. Pyro-phototronic effect has been extensively studied in ZnO-based photodetectors for possessing pyroelectricity of semiconducting ZnO. In general, pyro-phototronic effect plays a key role in promoting performance enhancement for ZnO-based photodetectors, such as improving responsivity and detectivity, shortening response/recovery time.[17]

ZnO is a unique material that exhibits semiconducting, piezoelectric, and pyroelectric multiple properties. The nanowire (NW) structure can enlarge the surface-to-volume ratio, which increases the interactive area between light and ZnO. Additionally, the light-trapping effect of the ZnO NW array can raise absorption by the multiple reflections between the single NW. It is beneficial to inspire the pyroelectric effect.

ZnO-based heterostructure (including Schottky junction, PN junction) photodetector attracts tremendous attention because the built-in potential in heterostructure can separate the photo-generated electron-hole pairs to achieve self-powered detection without consuming extra power. The heterostructure based on ZnO and perovskite is constructed to detect UV light.[11] This work introduces the long-overlooked pyroelectric effect induced by ultraviolet illumination to enhance the performance of photosensing. The spike current, which is called pyroelectric current, in the forwards and reverse direction, can be observed in Figure 2(*a*). The working mechanism of the photodetector is shown in Figure 2(*b*). Introduced into the pyro-phototronic effect, the response time is shortened from 5.4 s to 53 ms at the rising edge, and 8.9 s to 63 ms at the falling edge by five orders of magnitude. The detectivity and the responsivity are both improved by 322%. This self-powered photodetector designed by introducing pyroelectric effect achieves the ultrafast, high-sensitive detection for UV light. Further, the temperature dependence of pyro-phototronic effect is studied. The photoresponse current is improved over 500% owing to the enhanced pyro-phototronic effect at low temperature as the temperature decreases from 300 K to 77 K.[18] Temperature-dependence of the pyro-phototronic effect can also be observed in a p-Si/n-ZnO device fabricated by ZnO NWs grown on p-Si substrate.[19] The devices operate above room temperature (25 °C to 85 °C) and below room temperature (300 K to 77 K) to demonstrate the impact of external temperature. The current response of the devices is improved by over 1304% as the devices work at lower temperature than room temperature. In contrast, the current response boosts only by 532.6% when the working temperature is higher than room temperature.

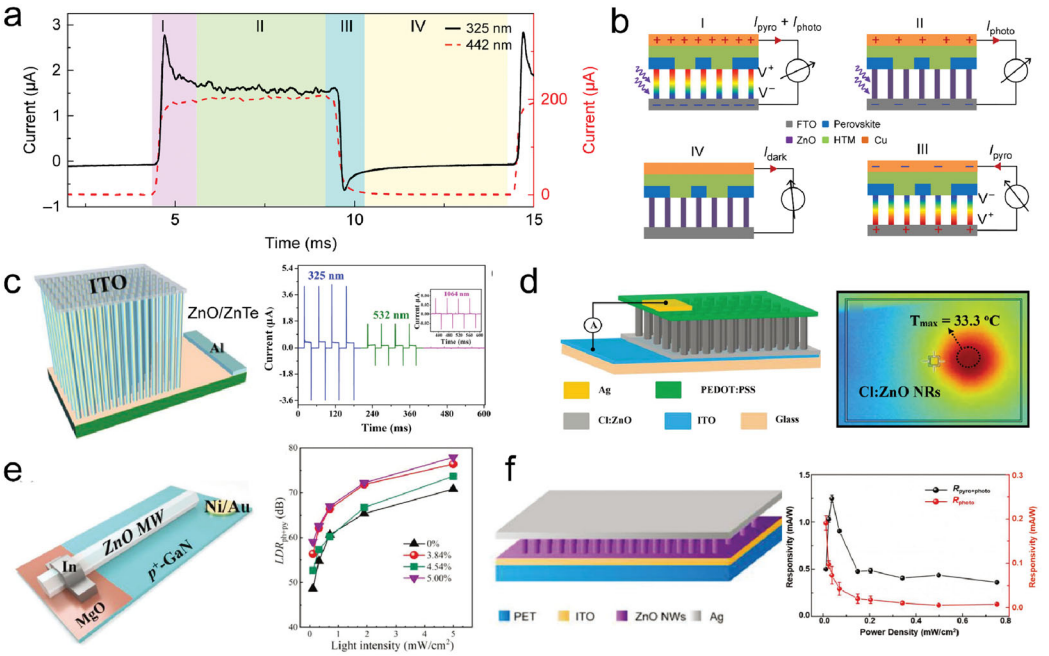

Figure 2. (*a*) I–t characteristics of the self-powered ZPH PDs under 325 nm and 442 nm laser illuminations. (*b*) Schematic illustration of the working mechanism of pyroelectric effect-combined photoexcitation processes, corresponding to the four stages labelled in a. (*c*) Structure of ZnO/ZnTe photodetector and I-t characteristics of ZnO/ZnTe photodetector under incident of different laser of wavelengths 325 nm (2.13 mW/cm^2), 532 nm (2.17 mW/cm^2) and 1064 nm (2.36 mW/cm^2) laser at zero bias under frequency of 20 Hz. (*d*) Structure of the Cl:ZnO NRs photodetector and thermal imaging of Cl:ZnO NRs. (*e*) Structure of the ZnO MW/p^+—GaN photodetector and corresponding linear dynamic range (LDR_{ph+py}) of the devices under different UV intensities. (*f*) Structure of the ZnO/Ag Schottky junction photodetector and corresponding photoresponsivity $R_{pyro+photo}$ and R_{photo} as a function of the power density.

Furthermore, the performance of the fabricated photodetectors declines slightly when temperature is increased between room temperature to 85 °C. The more temperature change is achieved (ΔT) by UV irradiation for a lower environmental temperature, leading to considerable pyroelectric current. When the temperature is above room temperature, suppression of the pyroelectric effect and the lattice vibration have an effect on the device. However, the carrier concentration and activity exactly go up. Thus, there is a comprehensive influence on the pyro-phototronic effect under high ambient temperature. Besides, the photoresponse current is frequency dependent. The photodetector based on p-n junction of p-Si and ZnO is constructed to investigate the frequency response.[20] The optimal response frequency of incident UV light is strongly dependent on the power density of incident UV light. For the UV light with low power density, the optimal response frequency is low, similarity, the optimal response frequency is high for the UV light with high power density. Additionally, pyroelectric current is dependance of bias voltage. The pyroelectric current decreases as the reverse bias increases.[21] The photoresponsivity of p-Si/n-ZnO photodetector is enhanced by up to 599% regarding to the relative changes of transient current in air. The response and recovery time are 19 μs and 22 μs, respectively, exhibiting the ultrafast response to 325 nm light. There is a ZnO/NiO/Si heterojunction photodetector that can selectively detect UV or visible light.[22] The ZnO/NiO/Si devices can detect UV irradiation for photoconduction effect of ZnO affected by oxygen adsorption and desorption, and the devices can response to visible light owing to photovoltaic effect of the heterojunction. NiO barrier layer in ZnO/NiO/Si heterojunction can significantly promote pyro-phototronic effect for effective reduction of the leakage current. ZnO-based photodetectors usually exhibit pyro-phototronic effect under UV illumination as the absorption of ZnO is within UV range. However, the devices

display pyro-phototronic effect under UV and visible illumination, attributing to the absorption of photons by the Si substrate.

Photodetectors that can detect broadband spectra from ultraviolet (UV) to near infrared (NIR) are beneficial for environmental surveillance, optical communication, and modern multispectral detection. Pyro-phototronic effect helps the self-powered photodetectors based on ZnO/ZnTe core-shell materials to realize broadband spectral detection (Figure 2(*c*)).[23] The devices exhibit different photoresponse behavior for 325 nm, 532 nm, and 1064 nm illumination for different interaction processes of pyro-phototronic effect. Pyrocurrent and photocurrent for 325 nm illumination are larger than those for 532 nm illumination owing to absorption of UV photons by both ZnTe and ZnO to produce greater temperature variations. Nevertheless, for 532 nm light, only ZnTe can absorb photons to produce I_{photo} and I_{pyro}. The devices display no I_{photo} as ZnO and ZnTe cannot absorb 1064 nm light. However, pyroelectric effect can significantly contribute to pyroelectric current as devices are illuminated by 1064 nm light. The transient responsivities for 325 nm, 532 nm, and 1064 nm lasers are calculated as 196.24, 77.46 and 1.11 mA/W, and the transient detectivities of 325 nm, 532 nm, and 1064 nm laser are calculated as 3.47×10^{12}, 1.36×10^{12}, and 1.95×10^{10} Jones, respectively.

All-oxide-based photodetectors are desired components for the emerging transparent optoelectronic devices. A transparent photodetector achieves ultrafast, self-powered UV detection through pyro-phototronic effect using ZnO and hole-selective V_2O_5.[24] ZnO shows appropriate band bending owing to hole-selective V_2O_5.[25] Transmittance of the device is high and greater than 70% in the visible region. More importantly, pyro-phototronic effect makes the photocurrent increase from 19 to 42 μA under illumination of 365 nm light (4 mW/cm^2). Thus, responsivity and detectivity are calculated as high as 4.4 mA/W and 7.35×10^{13} Jones, which are improved by 725%. Besides, 4 μs/16 μs for the rise/decay times are obtained in the photodetector. Translucent photodetector with the configuration of Cu_4O_3/ZnO/FTO is fabricated and the performance of this device is also enhanced by pyro-phototronic effect.[26] Transparent selective electrodes play key parts in enough exploitation of the pyro-phototronic effect. When the top electrode is only indium tin oxide (ITO), the device displays 69/80 μs photoresponse speeds, and corresponding responsivity and detectivity are obtained as 36 mA/W and 8.83×10^8 Jones, respectively. As silver nanowires (AgNWs) are used as the top electrode, the device displays a faster photoresponse speed of 60/70 μs, higher responsivity and detectivity of 262 mA/W and 3.66×10^9 Jones. Furthermore, the device with Ag NWs-coated ITO shows the highest rise and fall time of 7 and 10 μs and highest responsivity of 488 mA/W among the as-fabricated devices. The responsivity is enhanced by 1355 times compared to the original devices. A transparent NiO/ZnO heterojunction photodetector is also fabricated to take advantage of pyro-phototronic effect exhibiting high-performance ultraviolet detection.[27] The authors explore the influence of thermal treatment on ZnO films. Thermal treatment devices (300 K) display the higher performance as higher temperature has an effect on the distribution of pyroelectric potential within ZnO, contributing to the separation and transport of photo-generated electron-hole pairs and preventing from recombination. Thermal treatment devices show enhanced pyroelectric current by 1264.41%. Responsivity and detectivity of the thermal treatment devices display an increase over 5460% and 6063% compared to pristine devices. Moreover, the ultrafast response speed is also achieved in the devices as the rise time and decay time are 3.92 and 8.90 μs. Transparency of the devices can exceed 70% in the visible region.

However, the pyro-phototronic effect remains absent or extremely weak, so, it is not easy enough to be investigated, when it comes to the actual situation.[28–29] Even in the presence of pyroelectric effect, the magnitude of the rise in pyroelectric current and the speed of response show great variation.[13] Obviously, there are many other important internal physical factors that influence the pyroelectric effect. It is a rational method to dope pyroelectric materials to investigate detailed physical mechanisms of pyro-phototronic effect for displaying coupled process of

photovoltaic effect and pyroelectric effect. Doping electron donors or acceptors into semiconductors is an effective way to modulate electrical and thermal properties for the materials and then enabling high-performance electronic/optoelectronic devices.[30–31] Significant pyro-phototronic effect can be realized through tuning the charge carrier density in ZnO nanorods (NRs) by doping halogen elements (F, Cl, Br, I). One example is a device composed of PEDOT: PSS/Cl:ZnO NRs.[32] It is reported that photocurrent and pyroelectric current increase as sheet charge density increases in the ZnO with different doped elements. Hence, Cl:ZnO NRs devices display the highest photocurrent and pyroelectric current, compared to F: ZnO NRs, Br:ZnO NRs and I: ZnO NRs devices. Interestingly, the temperature of devices increases as sheet charge density goes up, when devices are irradiated under UV. Cl:ZnO NRs have the highest temperature of 33.3 °C (Figure 2(*d*)). So, pyro-phototronic effect can be enhanced by high sheet charge densities, and then merit parameters including response current, responsivity, specific detectivity, and external quantum efficiency are significantly high in the Cl:ZnO NRs photodetectors compared with other doped ZnO devices. A self-powered photodetector makes from Ga with different concentrations doped ZnO microwires (MWs) and p^+-GaN have also been used to investigate the influence of pyro-phototronic effect on performance (Figure 2(*e*)).[33] The devices with the highest concentration of the Ga dopant (5.00%) display highest responsivity (around 16 mA/W). Pyroelectric current gradually increases with the concentration of the Ga dopant rises. By contrast, photovoltaic current reaches the maximum at the concentration of 3.84% Ga dopant and then photovoltaic current decreases with Ga concentration further increasing. Depletion layer in the heterojunction devices decreases from 730 nm to 23 nm for the enhanced carrier concentration in ZnO:Ga MWs resulting in remarkable suppression of the photovoltaic current and photovoltaic sensitivity. As a result, pyroelectric current gradually dominates photocurrent with the increase of the Ga concentration. Pyro-phototronic effect promotes the reduction of decay time from 0.313 to 0.044 s. The total linear dynamic range (LDR_{ph+py}) is also boosted by doping Ga. The maximum LDR_{ph+py} is calculated as $\sim$ 75 dB (Figure 2(*e*)). The thermal imaging suggests that increasing Ga concentration in ZnO:Ga MWs can lead to UV absorption and higher photothermal conversion efficiencies. The devices with ZnO:Ga MWs (5.00%) show the highest temperature (27.9 °C) and hence pyroelectric current can increase dramatically. Another work also reports that pyro-phototronic effect promotes Ga doped ZnO MWs and Si heterojunction devices.[34] Maximum responsivity and detectivity are calculated as 0.185 A/W and 1.75×10^{12} Jones, respectively, for the single ZnO MW photodetector under illumination of 370 nm light. The response and recovery time are also decreased to about 499/412 μs. Moreover, ZnO:Ga MW/PEDOT:PSS heterostructure is also fabricated to detect UV light, displaying high performance for the dominated pyro-phototronic effect.[35] The photodetectors show responsivity $\sim$ 185 mA/W and detectivity $\sim 2.4 \times 10^{11}$ Jones under illumination of 370 nm laser. The devices also exhibit fast response, whose rise time and decay time are 212 μs and 387 μs.

Pyro-phototronic effect enhanced photodetectors can be modulated by plasmonic metal nanoparticles (NPs) to obtain tunability of sensitive light waveband. When P-Si/ZnO NWs photodetectors are inserted into a layer of plasmonic Au or Ag NPs between Si and ZnO, spectral insensitivity for the pyroelectric detectors is conquered.[36] The as-fabricated devices decorated with Ag or Au NPs at interface show the best current-response capability at 405 nm or 940 nm respectively. And the wavelength selection ratio is increased by a factor of 80. Response speed of the reported photodetectors can be highly improved through interface modification of plasmonic metal NP. In particular, Si/Ag/ZnO devices display ultrafast rise time of 20 μs under 405 nm light illumination at 825 Hz chopper frequency, whose rise time is 6 times higher than that of the Si/ZnO photodetector. Ultrafast optic-thermal coupling effect induced by LSPR and pyroelectric effect can account for this remarkable enhancement. Plasmonic Au NPs can also be used to enhance UV detection because they can absorb UV light and generate photo-generated electron-hole pairs interband transitions. So, there is a UV photodetector enhanced by pyro-phototronic

effect and plasmonic Au NPs. The device architecture has a layered configuration with Au NPs/ZnO/Au film where the sputter-deposited Au NPs and ZnO are photoactive layers. The photoactive layer can display significant absorption of UV light, leading to an increase of photocurrent at 365 nm. Although maximum responsivity and specific detectivity can be obtained as 4.68 A/W and 8.18×10^{11} Jones under a biased condition for the devices, the pyro-phototronic effect from the inherent pyroelectric property of the ZnO contributes to fast photoresponse. The fastest response time is 15 μs without external bias.

Near-infrared (NIR) photodetection has a wide range of applications including biomedical imaging, remote temperature sensing, and so on. Pyro-phototronic effect has been investigated in the field of NIR detection. Wang et al. fabricated flexible photodetectors by using a thin Si substrate with the thickness of dozens of micrometers to detect near-infrared light.[37] The near-infrared photodetector shows the high on/off photocurrent ratio up to 10^7 and the fast photoresponse a rise time of 15 μs and a fall time of 21 μs. NIR detection based on Si is compatible with state-of-the-art integration microcircuit and micro-nano fabrication technology. Recently, a self-powered, high-performance NIR photodetector is fabricated using p-Si, ultrathin aluminum trioxide (Al_2O_3) interlayer, and n-ZnO NWs.[38] The pyro-phototronic effect plays a key role in the excellent performance of the p-Si/Al_2O_3/n-ZnO NWs devices. Moreover, effective interfacial and optical modification by the Al_2O_3 interlayer also helps to improve the performance of the photodetectors. More photogenerated carriers achieve radiative recombination owing to Al_2O_3 nanolayer passivating interfacial defects. NIR absorption of Si can also be enhanced by the antireflection (AR) Al_2O_3 interlayer.[39] Pyroelectric potential can drive more electrons to tunnel through the barrier owing to the quantum tunneling effect induced by the Al_2O_3 layer. Hence, the NIR photodetector displays outstanding responsivity about 0.41 A/W and detectivity approaching 3.68×10^{12} Jones. Meanwhile, fast photoresponse speed is achieved in this photodetector as rise time is 15 μs and fall time is 21 μs. Chen et al. also fabricated three kinds of NIR photodetectors based on p-Si/n-ZnO NWs heterojunction (500 μm-Si/0.5 μm-ZnO device, 45 μm-Si/0.5 μm-ZnO device, and 45 μm-Si/2.5 μm-ZnO device).[40] Among the three kinds of devices, the 45 μm-Si/0.5 μm-ZnO devices display the best performances. Fast response/recovery time is 15 μs/21 μs. Responsivity and detectivity are as high as 164 mA/W and 8.78×10^{11} Jones respectively. More importantly, all devices display peak frequency response current due to resonance frequency arising on the occasion of light illumination. Resonance frequency $f_0 = 1/(\tau_E \tau_T)$, electric time constant $\tau_E = R_B(C_A + C_B)$ and thermal time constant $\tau_T = H/G$, where H, G, R_B, C_A and C_B are heat capacity, thermal conductivity, equivalent resistance, junction capacitance and external circuit capacitance, respectively.[41] This resonance frequency makes a difference in the way to regulating pyro-phototronic effect and then enhancing the performance of devices.

Previous devices generally consist of two layers including a pyroelectric semiconductor and another semiconductor or metal. This kind of device can only utilize polarization charges on one end of the semiconductor. Taking advantage of polarization charges induced on two ends of a pyroelectric semiconductor will make more excellent devices.[42] Pyro-phototronic effect has been investigated in a PEDOT: PSS/ZnO NWs/n-Si tri-layer heterojunction whose photoresponse performance to 648 nm laser illumination is significantly enhanced. responsivity increases from 0.823 (photovoltaic effect) to 22.054 mA/W (pyro-phototronic effect) under illumination (0.04 mW). Moreover, the photocurrent first increases and then reaches a plateau as the chopper frequency rises. The devices with short ZnO NWs have the more powerful current than those with long ZnO NWs. The authors also demonstrate a visible light communication system based on the as-fabricated devices that transmit and decrypt the encrypted light input signal. It is worthy of extensive attention to realize pyro-phototronic effect in this ZnO NWs based tri-layer heterojunction, which is beneficial for detecting ultrafast pulsed light and constructing light communication systems. Another tri-layer device with n-Si/p-SnO_x/n-ZnO can also make use of the pyro-phototronic effect to boost the photoresponse of the device.[43] When illuminated under a 405 nm laser

(36 mW/cm^2), the devices display peak responsivity and detectivity, 36.7 mA/W and 1.5×10^{11} Jones, at a chopper frequency of 400 Hz. Ultrafast response and recovery time are also obtained as 3 μs and 2 μs, respectively. Furthermore, under 650 nm laser illumination, the responsivity and detectivity can be obtained as 64.1 mA/W and 2.4×10^{11} Jones.

Most investigations for pyro-phototronic effect are major in p-n heterojunction devices. However, Schottky-contacted devices are also the excellent candidates for self-powered photodetection to investigate pyro-phototronic effect. Hence, a comprehensive pyro-phototronic effect is efficient to promote a self-powered and flexible ultraviolet PD based on the ZnO/Ag Schottky junction.[44] For the existing primary pyroelectric effect, the transient responsivity goes up and then decreases as light power density increases, obtaining peak responsivity of 1.25 mA/W, when the device is under illumination of 325 nm light with power density of 3.8×10^{-5} W/cm^2 (Figure 2(*f*)). And corresponding peak detectivity is obtained as 2.7×10^9 Jones. At the same time, the relatively high-temperature change will result in thermal deformation in ZnO crystal and then relative persist pyroelectric potential produces at the same direction. The charges at the junction reduce the height of Schottky barrier, leading to a reduction of the steady-state photocurrent with an increase in the power density. The photodetector displays a remarkable decrease in rise time and fall time decrease as the power density increases from 1.22×10^{-5} to 7.84×10^{-4} W/cm^2, which is the same as the behavior of a p–n junction photodetector. Our group also uses a Schottky-contacted Au@ZnO device to realize UV detection with an ultralow power density (68 nW/cm^2) by utilizing LSPR-inspired pyro-phototronic effect.[45] Responsivity significantly increases from 0 for the ZnO device to 0.485 mA/W for the Au/ZnO device. Similarly, detectivity is enhanced from 0 to 2.7×10^{11} Jones under illumination of 325 nm laser (68 nW/cm^2). The responsivity and detectivity show significant enhancement, increasing by over 3290% and over 3298% are obtained when power density increases to 170 nW/cm^2.

3. Pyro-phototronic effect in other semiconducting photodetectors

In addition to studying pyro-phototronic effect in ZnO-based photodetectors, other semiconductor materials are also used to develop pyro-phototronic effect enhanced photodetectors including SnS, CdS, $BaTiO_3$ (considered as semiconductors when fabricated by certain methods), some biomolecules, and so on. These materials have some advantages over ZnO in certain aspects, and the research on photodetectors based on these materials extends the function of pyro-phototronic effect such as broader detection band, ferroelectricity, stronger photoresponse, etc. For example, SnS has typic 2 D materials features and shows direct and controllable energy band gap values (1.3 eV–1.7 eV).[46] Moreover, the intrinsic SnS has a strong absorption coefficient (α, $> 5 \times 10^4$/cm) and high carrier mobility (10 000–38 000 cm^2/(V·s).[46] Of course, these materials have their failings compared to ZnO. For example, weak pyroelectric response and poor stability for some perovskite-based photodetectors.[47]

Vertically grown SnS layers have attracted much attention in photodetection. There is a broadband photodetector that can detect ultraviolet (365 nm) to near-infrared (850 nm) irradiation by using vertically grown SnS layers and a layer of Si.[48] SnS is a pyroelectric semiconductor like ZnO, so, pyro-phototronic effect can also promote the performance of SnS-based photodetectors. In this case, the photo current density rises from 100 μA/cm^2 of the devices without SnS layer to 470 μA/cm^2 with an SnS layer under 760 nm light illumination (7 mW/cm^2). Meanwhile, the SnS devices display ultrafast response/recovery time as approximately 12 μs/55 μs. Moreover, good responsivity and high detectivity are calculated as 13 mA/W and 3×10^{14} Jones under illumination with 7 mW/cm^2 760 nm light, showing increasing by 340% and 3960%, respectively. Applying an external electric field can counteract and suppress pyro-phototronic effect, resulting in an increase of photoresponse speed. So, the devices are measured photoresponse characteristics

under different external potentials. The results show that the pyro-phototronic effect can play a key role in enhancing the performance of devices.

CdS is also a semiconductor that has a noncentrosymmetric wurtzite structure with a direct intermediate bandgap (≈2.42 eV). CdS has received much attention in photodetection field.[49–50] Dai et al. constructed a self-powered flexible photodetector by forming a p-n heterojunction between p-Si and n-CdS NWs.[51] Broadband response for this self-powered photodetector can exceed the threshold of the intrinsic bandgap of Si and CdS, showing response for 325 nm to 1550 nm irradiation under zero bias with fast response speed. The pyro-phototronic effect here can actually enhance the performance of devices. The devices exhibit fast photoresponse under 325 nm laser illumination and the rise time and fall time are calculated as 245 and 277 μs, respectively. Meanwhile, the responsivity and detectivity for current from pyro-phototronic effect are 67.8 times and 17.4 times that of current only originating from photovoltaic effect. When illuminated with a 1060 nm laser, the devices display response/recovery time of 492 μs/654 μs. The responsivity and detectivity are both enhanced by 17.4 times. For a 1550 nm laser with the power density of 10 mW/cm^2, the peak responsivity and detectivity are 6.2 μA/W and 1.4×10^9 Jones, respectively. The rise time and fall time are calculated as 1.47 ms and 1.37 ms. The working mechanisms corresponding to different laser illuminations are carefully investigated. This pyro-phototronic effect enhanced Si/CdS photodetector will have widespread practical applications for compatibility with the traditional integrated circuit technology.

$BaTiO_3$ has a high pyroelectric coefficient of up to 16 nC/cm^{2}K. The excellent pyroelectric performance will make pyro-phototronic effect wonderful. Here, temperature variation-induced pyro-phototronic effect in polarized ferroelectric $BaTiO_3$ film is found to enhance the photocurrent of devices under illumination of 365 nm light.[52] The photoresponse characteristics of the polarized $BaTiO_3$ film also display a sharp current peak and a current plateau-like other pyroelectric material-based photodetectors. When applying an external heating temperature variation on the devices, the devices can output a current that is 30 times higher (0.6 mW/cm^2 illumination). Ferro-pyro-phototronic-effect can induce energy band bending at the interfaces of $BaTiO_3$ and ITO, which accounts for these results. Another work reports the temperature dependence of photocurrent and the influence of ferroelectric polarization under illumination of 405 nm light.[53] Co-planar interdigital ITO electrodes are utilized to improve charge collection ability and reduce recombination of electron-hole pairs.[54] The photocurrent of the devices increases by 121.9 ∼ 179.6% at low temperature (80–240 K) than that at room temperature. The device displays high responsivity and the maximum responsivity is 1.46×10^{-6} A/W at 220 K. Maximum detectivity can be obtained as 1.59×10^7 Jones at 240 K. Ferro-pyro-phototronic effect can account for the obvious enhancement of device performance. GaN, as one of the third-generation semiconductors, is usually used for UV light detection owing to its suitable bandgap (3.4 eV). The polarization of the ferroelectric material can enhance the change spontaneous polarization of GaN when UV light is illuminated. The self-powered photodetector based on $BaTiO_3$/GaN heterojunction is constructed to detect UV light by Zhang et al. [55] The schematic illustration and performance of self-powered photodetector are shown in Figure 3(*a*). With the cooling and prepolarization treatments, the photocurrent peak and plateau exhibit the improvement of over 1348% and 1052% (Figure 3(*a*) (right)). The response time of the pyroelectric current is shortened from 0.35 to 0.16 s. Ferroelectric $BaTiO_3$, which is the coexistence of photovoltaic, pyroelectric, and piezoelectric effects, is used to detect the light, temperature, and pressure (Figure 3(*b*)).[56–59] Ji et al. designed a device based on $BaTiO_3$ to detect the light. The schematic illustration of the device is shown in Figure 3(*b*).[60] The output current increases monotonously as increasing the power density of light as well as the temperature difference ΔT (Figure 3(*b*) (right)), indicating the device can monitor the power density of light and temperature variation by pro-phototronic effect.

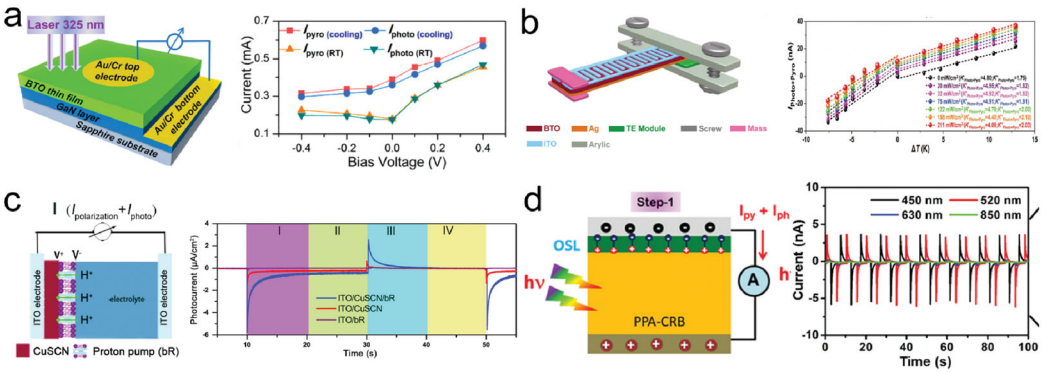

Figure 3. (*a*) Structure of the BTO/GaN photodetector and comparison of the I − t characteristics at different bias voltages with the maximum illumination power density under natural conditions. (*b*) Schematic diagram of the BTO-based sensor and dependence of output current on temperature difference ΔT under different light intensities. (*c*) A schematic illustration of the working mechanism of the polarization effect of the combined photoexcitation processes and one output period of photocurrent related to ITO/CuSCN, ITO/bR, and ITO/CuSCN/bR electrodes, divided into four stages, labeled as I, II, III, and IV. (*d*) Transient response of the PPA–CRB device at zero bias and short circuit on–off switching of the PPA–CRB-based device under the illumination of 450 nm, 520 nm, 630 nm and 850 nm light, with the intensity being fixed at 1 mW/cm^2 and at a frequency of 0.1 Hz.

Pyro-phototronic effect can contribute to multifunctional photoelectric devices based on the switchable ferroelectric photovoltaic (FPV) effect. Because FPV effect usually produces weak photocurrent. Jin et al. fabricated a near-ultraviolet photodetector consisting of Pt/$TmFeO_3$/Pt Schottky junction to investigate the switchable FPV and pyro-phototronic effect.[61] Poling electric field and light-induced pyroelectric potential will tune Schottky barrier height in the interface. Oxygen vacancies can be modulated by poling electric field and pyroelectric potential and then high oxygen vacancy concentration enhances the Schottky barrier, which significantly contributes to the separation of electron-hole pairs. Furthermore, $BiFeO_3$/Au/ZnO heterostructures are constructed to realize broad response wavelength from 360 nm to 1060 nm over the limitation of bandgap and investigate the regulation mechanism of integrating pyroelectric and photovoltaic effect from pyro-phototronic effect.[62] $BiFeO_3$/Au/ZnO devices show 1.4 times the short-circuit photocurrent density of $BiFeO_3$/ZnO devices under illumination of 405 nm light. Au NPs between $BiFeO_3$ and ZnO films make a difference in the enhancement of photoelectric performances and pyro-phototronic effect. Light-induced temperature variation and band alignment at interface result in pyroelectric and photovoltaic effect in $BiFeO_3$/Au/ZnO devices. Self-polarization phenomenon in $BiFeO_3$ and bent band will account for the corresponding photoelectric performances.

Coupling with the bio-semiconductor of bacteriorhodopsin (Br), Lv et al. constructed a bio p-n junction to investigate the self-corrosion and photoresponse performance.[63] The ITO/CuSCN/bR p-n junction emerges with the obvious feature of pyroelectric current when they are illuminated by a xenon arc lamp.(Figure 3(*c*)) Additionally, the photocurrent is enhanced by about 400% after integrating CuSCN with bR. This phenomenon is attributed to the electron-transition triggered proton transport mechanism. It is beneficial to understand the unique bionics design of light-driven ion pumps employing such semiconductors. Besides inorganic semiconductors, organic semiconductors of crystalline rubrene can also exhibit the pyro-phototronic effect.[64] Pyro-phototronic effect is found in a crystalline rubrene synthesized by plasma-based process (Figure 3(*d*)). The emergence of the photo-induced pyro-phototronic effect in a centrosymmetric rubrene crystal is solely owing to the induction of the surface polarization effect of the thin amorphous oxide layer formed over the crystalline film (Figure 3(*d*) (left)). The photoresponse performance of device based on crystalline rubrene is demonstrated by I-t dynamic response characteristics under alternative illumination of 450 nm, 520 nm, 630 nm, and 850 nm light (Figure 3(*d*) (right)).

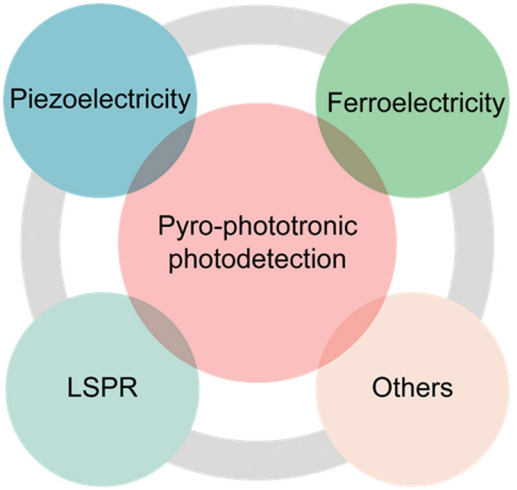

Figure 4. Schematic illustration among the piezoelectricity, ferroelectricity, LSPR, photoexcitation and pyro-phototronic photodetection.

4. Synergistic physical effects

As low carbon and pro-environment have become the focus of social issues, low power micro/nano sensors have also become targeted pursuit. In this case, devices that can response to multiple stimuli and convert them into electrical energy will make a difference. In order to achieve devices response to more external stimulation, it is significant to develop synergistic physical effects that enable devices with simpler structures to have more complex functions. Thus, synergistic physical effects make devices extensive application in public security, wearables, robotics, and internet of things. Achieving synergistic physical effects mainly relies on the multiple physical properties of materials and the organic combination of several materials. As descripted in Figure 4, pyro-phototronic effect, piezoelectricity, ferroelectricity, LSPR, and so on can combine with each other to realize synergistic physical effects and promote pyro-phototronic photodetection.

The pyro-phototronic effect has been investigated considerably in some pyroelectric materials as described above. These materials usually show piezoelectricity or ferroelectricity. Accordingly, it is a good opportunity to fabricate a photodetector with synergistic physical effects, which will promote the improvement of performance further. In the case of ZnO, coupling piezo-phototronic and pyro-phototronic effects can be achieved. Peng et al. constructed a self-powered PEDOT:PSS/ZnO photodetector to demonstrate that pyro-phototronic and the piezo-phototronic effect can be combined to significantly enhance the performance of photodetectors under illumination of 325 and 442 nm lasers.[65] Under −0.45% compressive strain, the photocurrent of the photodetector increases from 14.5 to 103 nA for 325 nm illumination (2.30 mW cm^{-2}), reaching over 600% improvement. The authors also conduct theoretical simulations to explain the coupled pyro-phototronic and piezo-phototronic effects through the finite element method. Moreover, the photoresponse performance of the photodetector can also be enhanced for 442 nm illumination as the pyro-phototronic effect and piezo-phototronic effect are combined. The photocurrent is improved, and rise time and fall time can be decreased dramatically (Figure 5(*a*)). The rise time decreases from 344.4 to 5.8 ms (over 5800% reduction) and fall time decreases from 344.4 to 5.8 ms (4200% reduction). This work has given certain comprehension on coupling the pyro-phototronic and the piezo-phototronic effect. $MAPbI_3$ ($MA = CH_3NH_3^+$), an organic–inorganic halide perovskite material, has also been demonstrated the possibility to enhance the performance of a photodetector by introducing pyro-phototronic and the piezo-phototronic effect. The photodetectors consist of $MAPbI_3$ single-crystal film/n-Si heterojunction.[47] First, maximum

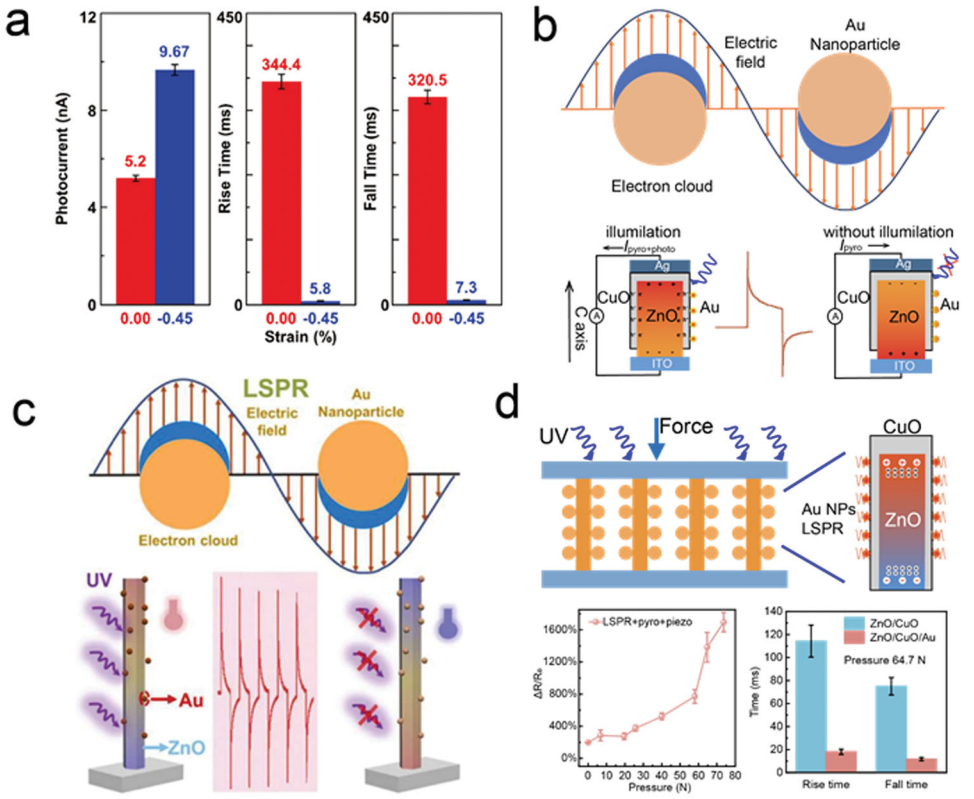

Figure 5. (*a*) Performance enhancement of the photodetectors to 442 nm 10 mW/cm^2 illumination by combining the pyro-phototronic and piezo-phototronic effects together, including the absolute photocurrent (I_{light}-I_{dark}), rise time, and fall time. (*b*) Schematic illustration of LSPR-inspired pyro-phototronic effect in ZnO/CuO/Au devices. (*c*) Schematic illustration of LSPR-enhanced pyro-phototronic effect in Ag-ZnO Schottky devices. (*d*) Self-powered photodetector based on ZnO/CuO/Au device enhanced by the coupling effect of LSPR, pyro-phototronic, and piezo-phototronic effect.

photoresponsivity of the photodetector approaches 1.5 mA/W under 780 nm illumination, for exploitation of the pyro-phototronic effect from $MAPbI_3$. Light-induced temperature change in $MAPbI_3$ film and then the pyroelectric charges distribute at the interface leading to downward bent energy band that will promote the separation of photogenerated electrons and holes. Second, when the devices are applied vertical pressures to involve piezo-phototronic effect, responsivity can be enhanced by more than 120% as the pressure increases from 0 to 155 kPa.

Some ferroelectric semiconductors are used in fabricating photodetectors. It is also useful to achieve pyro-phototronic effect in ferroelectric photodetectors. Here, a $BaTiO_3$-based flexible photodetector is fabricated and uses ferro-pyro-phototronic effect to enhance the photodetection performance.[58] Current peak and plateau in the device are 451.9% and 17.2% higher than those of an individual photovoltaic system. Energy band bending in the ferroelectric material contributes to the enhanced performance to detect 405 nm illumination.

There are many photodetectors that are fabricated with plasmonic NPs to realize an improvement in photodetection performance for using LSPR. Recently, the research on coupling pyro-phototronic effect has been proposed and this synergistic effect has a great impact on the performance of photodetectors. It is well-known that pyroelectric current is proportional to temperature variation.[66] Exactly, LSPR produces much transient thermal power to make a significant temperature increase fast.[67–69] Thus, LSPR can cooperate with the pyro-phototronic effect to enhance the pyroelectric photodetector. Especially the synergistic effect can play a key role when devices are used to detect a weak signal and even weak ultraviolet.

Hence, our group demonstrates a self-powered ZnO-based heterostructure photodetector to demonstrate the combination of pyro-phototronic effect and LSPR (Figure 5(*b*,*c*)).[45,70] Those self-powered photodetectors achieve fast and sensitive detection of UV when power density is 68 nW/cm^2. The performance of ZnO/CuO/Au device with LSPR-inspired pyro-phototronic effect is significantly higher than the ZnO/CuO device with only photovoltage effect. The optimal responsivity and detectivity under the same power density of UV at 325 nm are 1.4×10^{-4} A/W and 3.3×10^{11} Jones. Rise and fall time are remarkably shortened to about 10 ms. There is also another way to utilize LSPR and pyro-phototronic effect. Plasmonic metal nitrides prevail over traditional novel metal NPs in certain aspect including inexpensive price, high melting point, remarkable mechanical property, high electron mobility, compatibility for CMOS, and so on.[71–73] The excitonic-pyroelectric effect of ZnO crystal can cooperate with interband transition effect of TiN to achieve high sensitivity and ultrafast response speed in the photodetector.[74] The responsivity of the pristine device is near 12 mA/W. However, the ZnO/TiN device displays peak responsivity as 50 mA/W which is four times that of the pristine device. Fast response speed is achieved in the TiN/ZnO device. The rise time and decay time are 21 ± 2 μs and 27 ± 2 μs for the device. Finite difference time domain simulation is conducted to reveal the combination of interband transition of plasmonic TiN and pyroelectric ZnO.

Synergistic physical effect including LSPR, pyro-phototronic, and piezo-phototronic is also a good strategy to facilitate the improvement of a photodetector. More importantly, the study for this strategy may provide an in-depth understanding on the relationship and interaction among the three mechanisms. Recently, a self-powered photodetector based on ZnO/CuO/Au device was designed by our group to demonstrate the great enhancement by the coupled effect (Figure 5(*d*)).[75] Of course, the three effects can cooperate with each other well. For the low power density of 140 nW/cm^2, the photocurrent can be improved by ≈523% via the LSPR-inspired pyro-phototronic effect. Further, by introducing a pressure of 73.7 N to the photodetector, the enhancement of photocurrent can be increased by over 2900%.

5. Conclusions and perspectives

In summary, we have provided a widespread review of the construction of various high-performance photodetectors by utilizing pyro-phototronic effect. Pyro-phototronic effect combines pyroelectricity and excitation in a pyroelectric semiconductor material, which can modulate the separation, transportation, and extraction of photo-generated electron-hole pairs in optoelectronic processes. We have witnessed that pyro-phototronic effect enhanced photodetectors have achieved great progress in ZnO-based devices and then have extended to other materials such as CdS, SnS, perovskites, and some biomolecules. In this way, these photodetectors have realized fast response speeds, high responsivity, and detectivity for different detection wavelengths. Moreover, the pyro-phototronic effect has been used to combine with other physical properties including ferroelectricity, LSPR, and piezoelectricity to realize synergistic physical effects, which makes the photodetector more excellent in performance.

We describe recent advances in developing pyro-phototronic effect enhanced photodetectors to provide an overview of advances in common device structures with various materials, figure of merit, mechanisms for improvement, and more strategies for further enhanced performance. Although numerous research have centered on the pyro-phototronic effect enhanced photodetectors and got excellent results, some challenges and obstacles remain here. Firstly, more detailed mechanisms, such as electronic properties and carrier transport mechanisms, should be investigated, when hybrid systems are constructed involving piezoelectricity, ferroelectricity, and pyroelectricity. And then, it is essential to use these laws to realize practical applications using the optimal photodetectors. Secondly, most photodetectors with pyro-phototronic effect response

efficiently to UV. So, the devices for visible and near-infrared light will be more desired in the near future. Thirdly, it is also useful to study more extensive materials or develop some new materials to realize the pyro-phototronic. Especially, the biomolecular materials will be an important research object that can improve the biocompatibility of the devices, which will realize more prominent applications in vivo. This may provide more comprehension to this emerging field. Finally, more flexible self-powered photodetectors can be fabricated using pyro-phototronic effect and more Schottky-contacted photodetectors can be developed. Overall, future photodetectors may really have excellent performance by the investigation of pyro-phototronic and be used in practical production.

Disclosure statement

No potential conflict of interest was reported by the author(s).

Funding

The authors are thankful for the support provided by the National Natural Science Foundation of China (52002027, T2125003, 61875015), the Natural Science Foundation of Beijing Municipality (2214083, JQ20038, L212010), the Strategic Priority Research Program of the Chinese Academy of Sciences (XDA16021101) and the Youth Backbone Individual Project of Beijing Excellent Talents Training (Y9QNGG0501).

References

[1] Al-Jawhari, H.A. A review of recent advances in transparent p-type Cu2O-based thin film transistors. *Mater. Sci. Semicond. Process.* **2015**, *40*, 241–252. DOI: 10.1016/j.mssp.2015.06.063.

[2] Pal, B.N.; Robel, I.; Mohite, A.; Laocharoensuk, R.; Werder, D.J.; Klimov, V.I. High-sensitivity p–n junction photodiodes based on PbS nanocrystal quantum dots. *Adv. Funct. Mater.* **2012**, *22*, 1741–1748. DOI: 10.1002/adfm.201102532.

[3] Luo, L.; Wang, X.; Xie, C.; Li, Z.; Lu, R.; Yang, X.; Lu, J. One-dimensional CuO nanowire: Synthesis, electrical, and optoelectronic devices application. *Nanoscale. Res. Lett.* **2014**, *9*, 637. DOI: 10.1186/1556-276X-9-637.

[4] Boltar, K.O.; Burlakov, I.D.; Ponomarenko, V.P.; Filachev, A.M.; Salo, V.V. Solid-state photoelectronics of the ultraviolet range (review). *J. Commun. Technol. Electron.* **2016**, *61*, 1175–1185. DOI: 10.1134/S1064226916100041.

[5] Xie, Y.; Wei, L.; Wei, G.; Li, Q.; Wang, D.; Chen, Y.; Yan, S.; Liu, G.; Mei, L.; Jiao, J. A self-powered UV photodetector based on TiO2 nanorod arrays. *Nanoscale. Res. Lett.* **2013**, *8*, 188. DOI: 10.1186/1556-276X-8-188.

[6] Teng, F.; Hu, K.; Ouyang, W.; Fang, X. Photoelectric detectors based on inorganic p-type semiconductor materials. *Adv. Mater.* **2018**, *30*, 1706262. DOI: 10.1002/adma.201706262.

[7] Meng, J.; Li, Z. Schottky-contacted nanowire sensors. *Adv. Mater.* **2020**, *32*, 2000130. DOI: 10.1002/adma.202000130.

[8] Guan, X.; Yu, X.; Periyanagounder, D.; Benzigar, M.R.; Huang, J.K.; Lin, C.H.; Kim, J.; Singh, S.; Hu, L.; Liu, G.; et al. Recent progress in short- to long-wave infrared photodetection using 2D materials and heterostructures. *Adv. Opt. Mater.* **2021**, *9*, 2001708. DOI: 10.1002/adom.202001708.

[9] Deka Boruah, B. Zinc oxide ultraviolet photodetectors: Rapid progress from conventional to self-powered photodetectors. *Nanoscale Adv.* **2019**, *1*, 2059–2085. DOI: 10.1039/C9NA00130A.

[10] Ouyang, W.; Teng, F.; He, J.; Fang, X. Enhancing the photoelectric performance of photodetectors based on metal oxide semiconductors by charge-carrier engineering. *Adv. Funct. Mater.* **2019**, *29*, 1807672. DOI: 10.1002/adfm.201807672.

[11] Wang, Z.; Yu, R.; Pan, C.; Li, Z.; Yang, J.; Yi, F.; Wang, Z.L. Light-induced pyroelectric effect as an effective approach for ultrafast ultraviolet nanosensing. *Nat. Commun.* **2015**, *6*, 8401. DOI: 10.1038/ncomms9401.

[12] Hu, X.; Li, X.; Li, G.; Ji, T.; Ai, F.; Wu, J.; Ha, E.; Hu, J. Recent progress of methods to enhance photovoltaic effect for self-powered heterojunction photodetectors and their applications in inorganic low-dimensional structures. *Adv. Funct. Mater.* **2021**, *31*, 2011284. DOI: 10.1002/adfm.202011284.

[13] Xu, Z.; Zhang, Y.; Wang, Z. ZnO-based photodetector: From photon detector to pyro-phototronic effect enhanced detector. *J. Phys. D: Appl. Phys.* **2019**, *52*, 223001. DOI: 10.1088/1361-6463/ab0728.
[14] Wei, C.; Xu, J.; Shi, S.; Cao, R.; Chen, J.; Dong, H.; Zhang, X.; Yin, S.; Li, L. Self-powered visible-blind UV photodetectors based on p-NiO nanoflakes/n-ZnO nanorod arrays with an MgO interfacial layer. *J. Mater. Chem. C.* **2019**, *7*, 9369–9379. DOI: 10.1039/C9TC01179J.
[15] Chen, X.; Liu, K.; Zhang, Z.; Wang, C.; Li, B.; Zhao, H.; Zhao, D.; Shen, D. Self-powered solar-blind photodetector with fast response based on Au/*β*-Ga2O3 nanowires array film schottky junction. *Am. Chem. Soc. Appl. Mater. Interfaces* **2016**, *8*, 4185–4191. DOI: 10.1021/acsami.5b11956.
[16] Li, Z.; Qiao, H.; Guo, Z.; Ren, X.; Huang, Z.; Qi, X.; Dhanabalan, S.C.; Ponraj, J.S.; Zhang, D.; Li, J.; et al. High-performance photo-electrochemical photodetector based on liquid-exfoliated few-layered InSe nanosheets with Eenhanced stability. *Adv. Funct. Mater.* **2018**, *28*, 1705237. DOI: 10.1002/adfm.201705237.
[17] Ouyang, W.; Chen, J.; Shi, Z.; Fang, X. Self-powered UV photodetectors based on ZnO nanomaterials. *Appl. Phys. Rev.* **2021**, *8*, 031315. DOI: 10.1063/5.0058482.
[18] Peng, W.; Yu, R.; Wang, X.; Wang, Z.; Zou, H.; He, Y.; Wang, Z.L. Temperature dependence of pyro-phototronic effect on self-powered ZnO/perovskite heterostructured photodetectors. *Nano Res.* **2016**, *9*, 3695–3704. DOI: 10.1007/s12274-016-1240-5.
[19] Dong, J.; Wang, Z.; Wang, X.; Wang, Z.L. Temperature dependence of the pyro-phototronic effect in self-powered p-Si/n-ZnO nanowires heterojuncted ultraviolet sensors. *Nano Today* **2019**, *29*, 100798. DOI: 10.1016/j.nantod.2019.100798.
[20] Feng, Y.; Zhang, Y.; Wang, Y.; Wang, Z. Frequency response characteristics of pyroelectric effect in p-n junction UV detectors. *Nano Energy* **2018**, *54*, 429–436. DOI: 10.1016/j.nanoen.2018.10.022.
[21] Wang, Z.; Yu, R.; Wang, X.; Wu, W.; Wang, Z.L. Ultrafast response p-Si/n-ZnO heterojunction ultraviolet detector based on pyro-phototronic effect. *Adv. Mater.* **2016**, *28*, 6880–6886. DOI: 10.1002/adma.201600884.
[22] Yin, B.; Zhang, H.; Qiu, Y.; Luo, Y.; Zhao, Y.; Hu, L. The light-induced pyro-phototronic effect improving a ZnO/NiO/Si heterojunction photodetector for selectively detecting ultraviolet or visible illumination. *Nanoscale* **2017**, *9*, 17199–17206. DOI: 10.1039/c7nr06037h.
[23] You, D.; Xu, C.; Zhang, W.; Zhao, J.; Qin, F.; Shi, Z. Photovoltaic-pyroelectric effect coupled broadband photodetector in self-powered ZnO/ZnTe core/shell nanorod arrays. *Nano Energy* **2019**, *62*, 310–318. DOI: 10.1016/j.nanoen.2019.05.050.
[24] Kumar, M.; Patel, M.; Nguyen, T.T.; Kim, J.; Yi, J. High-performing ultrafast transparent photodetector governed by the pyro-phototronic effect. *Nanoscale* **2018**, *10*, 6928–6935. DOI: 10.1039/c7nr09699b.
[25] Kim, H.; Chauhan, K.R.; Kim, J.; Choi, E.H. Flexible vanadium oxide film for broadband transparent photodetector. *Appl. Phys. Lett.* **2017**, *110*, 101907. DOI: 10.1063/1.4977426.
[26] Abbas, S.; Kumar, M.; Kim, D.W.; Kim, J. Translucent photodetector with blended nanowires–metal oxide transparent selective electrode utilizing photovoltaic and pyro-phototronic coupling effect. *Small* **2019**, *15*, 1804346. DOI: 10.1002/smll.201804346.
[27] Rana, A.K.; Kumar, M.; Ban, D.K.; Wong, C.P.; Yi, J.; Kim, J. Enhancement in performance of transparent p-NiO/n-ZnO heterojunction ultrafast self-powered photodetector via pyro-phototronic effect. *Adv. Electron. Mater.* **2019**, *5*, 1900438. DOI: 10.1002/aelm.201900438.
[28] Song, Z.; Zhou, H.; Ye, C.; Yang, L.; Xue, M.; Mei, J.; Wang, H. Surface treatment for schottky barrier photodetector based on Au/GaZnO nanorods/Au structure. *Mater. Sci. Semicond. Process.* **2017**, *64*, 101–108. DOI: 10.1016/j.mssp.2017.03.023.
[29] Zheng, X.; Sun, Y.; Qin, H.; Ji, Z.; Chi, H. Interface engineering on ZnO/Au based schottky junction for enhanced photoresponse of UV detector with TiO2 inserting layer. *J. Alloys Compd.* **2020**, *816*, 152537. DOI: 10.1016/j.jallcom.2019.152537.
[30] Shinde, S.S.; Shinde, P.S.; Oh, Y.W.; Haranath, D.; Bhosale, C.H.; Rajpure, K.Y. Structural, optoelectronic, luminescence and thermal properties of Ga-doped zinc oxide thin films. *Appl. Surf. Sci.* **2012**, *258*, 9969–9976. DOI: 10.1016/j.apsusc.2012.06.058.
[31] Saha, S.K.; Rahman, M.A.; Sarkar, M.R.H.; Shahjahan, M.; Khan, M.K.R. Effect of Co doping on structural, optical, electrical and thermal properties of nanostructured ZnO thin films. *J. Semicond.* **2015**, *36*, 033004. DOI: 10.1088/1674-4926/36/3/033004.
[32] Deka, B.B.; Naidu, M.S.; Nandi, S.; Misra, A. Doping controlled pyro-phototronic effect in self-powered zinc oxide photodetector for enhancement of photoresponse. *Nanoscale* **2018**, *10*, 3451–3459. DOI: 10.1039/c7nr08125a.
[33] Wan, P.; Jiang, M.; Xu, T.; Liu, Y.; Fang, X.; Kan, C. Doping concentration influenced pyro-phototronic effect in self-powered photodetector based on Ga-incorporated ZnO microwire/p+-GaN heterojunction. *Adv. Opt. Mater.* **2022**, *10*, 2101851. DOI: 10.1002/adom.202101851.

[34] Dai, R.; Liu, Y.; Wu, J.; Wan, P.; Zhu, X.; Kan, C.; Jiang, M. Self-powered ultraviolet photodetector based on an n-ZnO:Ga microwire/p-Si heterojunction with the performance enhanced by a pyro-phototronic effect. *Opt. Express.* **2021**, *29*, 30244–30258. DOI: 10.1364/OE.439587.

[35] Wan, P.; Jiang, M.; Xu, T.; Liu, Y.; Kan, C. High-mobility induced high-performance self-powered ultraviolet photodetector based on single ZnO microwire/PEDOT:PSS heterojunction via slight ga-doping. *J. Mater. Sci. Technol.* **2021**, *93*, 33–40. DOI: 10.1016/j.jmst.2021.03.047.

[36] Zhu, Y.; Wang, B.; Deng, C.; Wang, Y.; Wang, X. Photothermal-pyroelectric-plasmonic coupling for high performance and tunable band-selective photodetector. *Nano Energy* **2021**, *83*, 105801. DOI: 10.1016/j.nanoen.2021.105801.

[37] Wang, X.; Dai, Y.; Liu, R.; He, X.; Li, S.; Wang, Z.L. Light-triggered pyroelectric nanogenerator based on a pn-junction for self-powered near-infrared photosensing. *ACS Nano* **2017**, *11*, 8339–8345. DOI: 10.1021/acsnano.7b03560.

[38] Wang, B.; Zhu, Y.; Dong, J.; Jiang, J.; Wang, Q.; Li, S.; Wang, X. Self-powered, superior high gain silicon-based near-infrared photosensing for low-power light communication. *Nano Energy* **2020**, *70*, 104544. DOI: 10.1016/j.nanoen.2020.104544.

[39] Szeghalmi, A.; Helgert, M.; Brunner, R.; Heyroth, F.; Gösele, U.; Knez, M. Atomic layer deposition of Al2O3 and TiO2 multilayers for applications as bandpass filters and antireflection coatings. *Appl. Opt.* **2009**, *48*, 1727–1732. DOI: 10.1364/ao.48.001727.

[40] Chen, L.; Wang, B.; Dong, J.; Gao, F.; Zheng, H.; He, M.; Wang, X. Insights into the pyro-phototronice Effect in p-Si/n-ZnO nanowires heterojunction toward high-performance near-infrared photosensing. *Nano Energy* **2020**, *78*, 105260. DOI: 10.1016/j.nanoen.2020.105260.

[41] Whatmore, R.W. Pyroelectric devices and materials. *Rep. Prog. Phys.* **1986**, *49*, 1335–1386. DOI: 10.1088/0034-4885/49/12/002.

[42] Li, F.; Peng, W.; Pan, Z.; He, Y. Optimization of Si/ZnO/PEDOT:PSS tri-layer heterojunction photodetector by piezo-phototronic effect using both positive and negative piezoelectric charges. *Nano Energy* **2018**, *48*, 27–34. DOI: 10.1016/j.nanoen.2018.03.025.

[43] Silva, J.P.B.; Vieira, E.M.F.; Gwozdz, K.; Kaim, A.; Goncalves, L.M.; MacManus-Driscoll, J.L.; Hoye, R.L.Z.; Pereira, M. High-performance self-powered photodetectors achieved through the pyro-phototronic effect in Si/SnO_x/ZnO heterojunctions. *Nano Energy* **2021**, *89*, 106347. DOI: 10.1016/j.nanoen.2021.106347.

[44] Wang, Y.; Zhu, L.; Feng, Y.; Wang, Z.; Wang, Z.L. Comprehensive pyro-phototronic effect enhanced ultraviolet detector with ZnO/Ag schottky junction. *Adv. Funct. Mater.* **2019**, *29*, 1807111. DOI: 10.1002/adfm.201807111.

[45] Meng, J.; Li, Q.; Huang, J.; Pan, C.; Li, Z. Self-powered photodetector for ultralow power density UV sensing. *Nano Today* **2022**, *43*, 101399. DOI: 10.1016/j.nantod.2022.101399.

[46] Patel, M.; Kim, H.; Kim, J. Wafer-scale production of vertical SnS multilayers for high-performing photoelectric devices. *Nanoscale* **2017**, *9*, 15804–15812. DOI: 10.1039/C7NR03370B.

[47] Yang, Z.; Wang, H.; Guo, L.; Zhou, Q.; Gu, Y.; Li, F.; Qiao, S.; Pan, C.; Wang, S. A self-powered photodetector based on $MAPbI_3$ single-crystal film/n-Si heterojunction with broadband response enhanced by pyro-phototronic and piezo-phototronic effects. *Small* **2021**, *17*, 2101572. DOI: 10.1002/smll.202101572.

[48] Kumar, M.; Patel, M.; Kim, J.; Lim, D. Enhanced broadband photoresponse of a self-powered photodetector based on vertically grown SnS layers via the pyro-phototronic effect. *Nanoscale* **2017**, *9*, 19201–19208. DOI: 10.1039/c7nr07120e.

[49] Deng, K.; Li, L. CdS nanoscale photodetectors. *Adv. Mater.* **2014**, *26*, 2619–2635. DOI: 10.1002/adma.201304621.

[50] Dai, Y.; Wang, X.; Peng, W.; Zou, H.; Yu, R.; Ding, Y.; Wu, C.; Wang, Z.L. Largely improved near-infrared silicon-photosensing by the piezo-phototronic effect. *ACS Nano.* **2017**, *11*, 7118–7125. DOI: 10.1021/acsnano.7b02811.

[51] Dai, Y.; Wang, X.; Peng, W.; Xu, C.; Wu, C.; Dong, K.; Liu, R.; Wang, Z.L. Self-powered Si/CdS flexible photodetector with broadband response from 325 to 1550 nm based on pyro-phototronic effect: An approach for photosensing below bandgap energy. *Adv. Mater.* **2018**, *30*, 1705893. DOI: 10.1002/adma.201705893.

[52] Zhao, K.; Ouyang, B.; Yang, Y. Enhancing photocurrent of radially polarized ferroelectric BaTiO3 materials by ferro-pyro-phototronic effect. *Science* **2018**, *3*, 208–216. DOI: 10.1016/j.isci.2018.04.016.

[53] Ma, N.; Yang, Y. Boosted photocurrent via cooling ferroelectric BaTiO3 materials for self-powered 405 nm light detection. *Nano Energy* **2019**, *60*, 95–102. DOI: 10.1016/j.nanoen.2019.03.036.

[54] Ma, N.; Yang, Y. Boosted photocurrent in ferroelectric $BaTiO_3$ materials via two dimensional planar-structured contact configurations. *Nano Energy* **2018**, *50*, 417–424. DOI: 10.1016/j.nanoen.2018.05.069.

[55] Zhang, Y.; Chen, J.; Zhu, L.; Wang, Z.L. Self-powered high-responsivity photodetectors enhanced by the pyro-phototronic effect based on a $BaTiO_3$/GaN heterojunction. *Nano Lett.* **2021**, *21*, 8808–8816. DOI: 10.1021/acs.nanolett.1c03171.

[56] Ji, Y.; Zhang, K.; Wang, Z.L.; Yang, Y. Piezo–pyro–photoelectric effects induced coupling enhancement of charge quantity in $BaTiO_3$ materials for simultaneously scavenging light and vibration energies. *Energy Environ. Sci.* **2019**, *12*, 1231–1240. DOI: 10.1039/C9EE00006B.

[57] Ma, N.; Yang, Y. Enhanced self-powered UV photoresponse of ferroelectric BaTiO3 materials by pyroelectric effect. *Nano Energy* **2017**, *40*, 352–359. DOI: 10.1016/j.nanoen.2017.08.043.

[58] Zhao, K.; Ouyang, B.; Bowen, C.R.; Yang, Y. Enhanced photocurrent via ferro-pyro-phototronic effect in ferroelectric BaTiO3 materials for a self-powered flexible photodetector system. *Nano Energy* **2020**, *77*, 105152. DOI: 10.1016/j.nanoen.2020.105152.

[59] Ma, N.; Zhang, K.; Yang, Y. Photovoltaic–pyroelectric coupled effect induced electricity for self-powered photodetector system. *Adv. Mater.* **2017**, *29*, 1703694. DOI: 10.1002/adma.201703694.

[60] Ji, Y.; Wang, Y.; Yang, Y. Photovoltaic–pyroelectric–piezoelectric coupled effect induced electricity for self-powered coupled sensing. *Adv. Electron. Mater.* **2019**, *5*, 1900195. DOI: 10.1002/aelm.201900195.

[61] Jin, L.; He, Y.; Zhang, D.; Zhang, H.; Wei, M.; Zhong, Z. Near-ultraviolet photodetector based on hexagonal TmFeO3 ferroelectric semiconductor thin film with photovoltaic and pyroelectric effects. *APL Mater.* **2019**, *7*, 121105. DOI: 10.1063/1.5128702.

[62] Zhang, Y.; Su, H.; Li, H.; Xie, Z.; Zhang, Y.; Zhou, Y.; Yang, L.; Lu, H.; Yuan, G.; Zheng, H. Enhanced photovoltaic-pyroelectric coupled effect of BiFeO3/Au/ZnO heterostructures. *Nano Energy* **2021**, *85*, 105968. DOI: 10.1016/j.nanoen.2021.105968.

[63] Lv, Y.; Liang, D.; Lu, S.; Aurbach, D.; Xiang, Y. Unidirectional electron injection and accelerated proton transport in bacteriorhodopsin based bio-p-n junctions. *Biosens. Bioelectron.* **2020**, *173*, 112811. DOI: 10.1016/j.bios.2020.112811.

[64] Gogoi, D.; Hussain, A.A.; Biswasi, S.; Pal, A.R. Crystalline rubrenevia a novel process and realization of a pyro-phototronic device with a rubrene-based film. *J. Mater. Chem. C.* **2020**, *8*, 6450–6460. DOI: 10.1039/D0TC00857E.

[65] Peng, W.; Wang, X.; Yu, R.; Dai, Y.; Zou, H.; Wang, A.C.; He, Y.; Wang, Z.L. Enhanced performance of a self-powered organic/inorganic photodetector by pyro-phototronic and piezo-phototronic effects. *Adv. Mater.* **2017**, *29*, 1606698. DOI: 10.1002/adma.201606698.

[66] Stewart, J.W.; Vella, J.H.; Li, W.; Fan, S.; Mikkelsen, M.H. Ultrafast pyroelectric photodetection with on-chip spectral filters. *Nat. Mater.* **2020**, *19*, 158–162. DOI: 10.1038/s41563-019-0538-6.

[67] Yu, G.; Qian, J.; Zhang, P.; Zhang, B.; Zhang, W.; Yan, W.; Liu, G. Collective excitation of plasmon-coupled Au-nanochain boosts photocatalytic hydrogen evolution of semiconductor. *Nat. Commun.* **2019**, *10*, 4912. DOI: 10.1038/s41467-019-12853-8.

[68] Chen, X.; Chen, Y.; Yan, M.; Qiu, M. Nanosecond photothermal effects in plasmonic nanostructures. *ACS Nano.* **2012**, *6*, 2550–2557. DOI: 10.1021/nn2050032.

[69] Govorov, A.O.; Richardson, H.H. Generating heat with metal nanoparticles. *Nano Today* **2007**, *2*, 30–38. DOI: 10.1016/S1748-0132(07)70017-8.

[70] Li, Q.; Meng, J.; Huang, J.; Li, Z. Plasmon-induced pyro-phototronic effect enhancement in self-powered UV–vis detection with a ZnO/CuO p–n junction device. *Adv. Funct. Materials* **2022**, *32*, 2108903. DOI: 10.1002/adfm.202108903.

[71] Naik, G.V.; Shalaev, V.M.; Boltasseva, A. Alternative plasmonic materials: Beyond gold and silver. *Adv. Mater.* **2013**, *25*, 3264–3294. DOI: 10.1002/adma.201205076.

[72] Naik, G.V.; Schroeder, J.L.; Ni, X.; Kildishev, A.V.; Sands, T.D.; Boltasseva, A. Titanium nitride as a plasmonic material for visible and near-infrared wavelengths. *Opt. Mater. Express* **2012**, *2*, 478–489. DOI: 10.1364/OME.2.000478.

[73] Patsalas, P.; Kalfagiannis, N.; Kassavetis, S. Optical properties and plasmonic performance of titanium nitride. *In Materials* **2015**, *8*, 3128–3154. DOI: 10.3390/ma8063128.

[74] Podder, S.; Bora, J.; Thakur, S.; Gogoi, D.; Basumatary, B.; Borah, S.M.; Adhikary, N.C.; Pal, A.R. Interband transition in plasmonic titanium nitride and its contribution towards ZnO based pyro-phototronic application. *Mater. Chem. Phys.* **2022**, *275*, 125290. DOI: 10.1016/j.matchemphys.2021.125290.

[75] Li, Q.; Huang, J.; Meng, J.; Li, Z. Enhanced performance of a self-powered ZnO photodetector by coupling LSPR-inspired pyro-phototronic effect and piezo-phototronic effect. *Adv. Opt. Mater.* **2022**, 2102468. DOI: 10.1002/adom.202102468.